Kashf Journal of Multidisciplinary Research
Vol:02 - Issue09(2025)
P-ISSN: 3007-1992 E-ISSN: 3007-200X
https://kjmr.com.pk

DYNAMIC ANALYSIS OF SINGLE ACTIVE BRIDGE DC-DC CONVERTER DURING LINE VARIATION

[1]Dr. Saad Khan Baloch*, [2]Dr. Abdul Hameed Soomro, [3]Numan Ali, [4]Prof. Dr. Abdul Sattar Larik, [5]Prof. Dr. Mukhtiar Ahmed Mahar

[1]Department of Electrical Engineering, Isra University Hyderabad, Sindh, Pakistan

[2]Department of Electrical Engineering, The University of Larkano, Sindh, Pakistan

[3]BS Electrical Engineering, COMSATS University Islamabad Wah Campus & MS Electrical Engineering, Department of Electrical Engineering, Abasyn University Peshawar, Department: EE

[4, 5]Department of Electrical Engineering, Mehran University of Engineering and Technology Jamshoro, Sindh, Pakistan

****Corresponding Author:*** saad.baloch@isra.edu.pk

Article Info

Abstract

With the growing need for high-efficiency power conversion in renewable energy, transport and grid applications, research on innovative DC-DC converter topologies has been accelerated. Among these, Single Active Bridge (SAB) converter has received much attention for its structural simplicity, compactness, and low switching losses. However, the performance of the resulting system is limited when controlled using conventional proportional-integral (PI) control schemes due to the presence of oscillations, voltage overshoot and poor dynamic performance under line disturbances. This paper reports a comprehensive dynamic analysis of SAB converter under step-to-step line variation using a cascaded control strategy with inner current loop and outer voltage loop. The converter is modeled in state-space averaging, the transfer functions of voltage and current loops are derived, and then the model is simulated in MATLAB/Simulink under different supply conditions. As shown in Figures 8 and 9 with the summary of results in Table 1, the cascaded control has a smaller peak-to-peak overshoot and better settling time than the single-loop PI control because the maximum overshoot is 25 V and 27 V for the line increase and line drop tests, respectively. Furthermore, SAB converter applications in renewable energy systems, solid-state transformers, electric vehicles, and future HVDC/MVDC networks are also discussed to show the versatility of the topology. The results show that cascaded control increases the robustness of SAB converters against the perturbation, therefore these converters are better candidates for the next generation high power and renewable energy applications.

Keywords:

SAB Converter, Cascaded Control, Line Variation, State-Space Modeling, PI Controller, Renewable Energy, HVDC, MVDC, Solid-State Transformer, Electric Vehicle

1. INTRODUCTION

With the tremendous development of power electronics, modern industrial, commercial and domestic systems have been revolutionized for efficiency, compactness and reliability. A DC-DC converter is one of the most important components of such systems, as it can efficiently convert voltage levels while delivering stable power to the loads. Unlike linear regulators, DC-DC converters based on switching technology have higher energy efficiency and more flexibility for meeting the power requirements of demanding applications such as microelectronics, as well as serving large scale renewable energy grids [1-3]. The ability of these converters to scale up and down voltage and isolate circuits while minimizing energy losses makes them invaluable to modern power electronic design.

The single most obvious driver for the increasing use of DC-DC converters is the need for high-frequency switching to allow higher power density, smaller passive element sizes and better transient response. In addition, the magnitude and weight of inductors and capacitors may be minimized by increasing the frequency, which is necessary in applications where a small sized and lightweight system is needed, for example in electric vehicles and portable electronics [5,6]. However, with the trend towards high frequency operation, new challenges such as higher switching and conduction losses, electromagnetic interference (EMI) and thermal management issues are added [7]. Furthermore, parasitic components of the semiconductor devices and circuit geometries cause increased switching transients that lead to low efficiency and potential reliability problems [8]. Therefore, despite the advantages associated with operation at higher frequency, it requires new topologies and control methods to mitigate these losses in performance [9].

It is also emphasized that DC-DC converter has a wide range of applications in the modern technologies. In the Internet of Things (IoT) space, these converters are critical components in powering low-voltage sensors, microcontrollers, and communication modules where efficiency directly translates to device life. In addition, in industrial robots and automation, DC-DC converters are used for motors and actuators, which allows for precise and stable voltage regulation, ensuring reliability and accuracy in high-speed movements. In renewable energy systems, especially solar photovoltaic (PV) array and wind turbine system, the DC-DC converter is applied for maximum power point tracking (MPPT) to obtain the appropriate power under different environmental conditions [12]. Moreover, high efficiency DC/DC power supplies are extensively used in data centers and cloud computing infrastructure for stable operation in the event of huge power load, and even a minor efficiency improvement results in huge cost and energy savings [13]. DC-DC converters have found their way into many different types of applications, and are a vital component of consumer and large industry systems.

Within this large family of topologies, the Single Active Bridge (SAB) DC-DC converter has emerged as an attractive topology owing to its structural simplicity, low component number and possibly high efficiency [14]. SAB converters have low switching losses and conduction losses, compared with more complex converters such as the Dual Active Bridge (DAB). However, in spite of these merits, SAB converters have poor dynamic responses in terms of input line changes and load disturbances. Under these conditions, voltage overshoots, long settling times and oscillations are manifested which directly influence the stability and efficiency of the overall system [15]. Although traditional Proportional-

Integral (PI) control is being widely used, it is proved that the PI controller is not sufficient for compensating the nonlinearity of SAB converter, particularly under the high frequency switching controlling [16]. However, increased demands for advanced and robust control strategies to suppress transient perturbations, oscillations and improve the dynamic response are continuously growing.

Therefore, this study can be regarded as a contribution to dynamic analysis of SAB converters under the conditions of line variation using a cascaded control scheme. Cascade control is used to achieve a more stable and better disturbance rejection than the single loop PI controller by combining the inner fast current loop and outer voltage regulation loop. Beside the performance improvement, solving those problems will also greatly increase the credibility of SAB converters for strategic applications like renewable integration, electric vehicles, and future high voltage DC.

3. Literature Review

3.1 DC-DC Converter Topologies

A variety of DC-DC converter topologies have been researched over the past two decades in order to achieve better performance, higher power density, and lower system cost. The most common are the buck and boost converters which are at the core of many advanced power conversion systems. The buck converter is used to step down the voltage with a relatively low switching loss, while the boost converter is used to step up the input voltage to desirable levels for many applications such as automotive electronics, and integration with renewable sources [20]. In more complicated applications, bidirectional converters have been getting popular because they can allow power transfer in both directions and this property is required for energy storage systems, hybrid electric vehicles and distributed renewable generation [21]. Multiple-output DC/DC converters, however, are attracting attention in compact systems, e.g., central processing unit (CPU), portable electronics, and communication apparatus in which miniaturization and efficiency are important requirements [22].

In renewable energy systems, DC/DC converters are the core for efficient power conversion. In solar PV arrays they provide the required voltage regulation and interface to maximum power point tracking (MPPT) algorithms. In electric vehicles (EVs), converters form the interface between the battery pack and the traction systems and provide steady operation under the load conditions that rapidly change over time [23]. The scope of the converter applications has further expanded with the advent of high-voltage and medium-voltage DC (HVDC/MVDC) systems, which offer the benefits of galvanic isolation and active power flow control as well as stabilization of the DC microgrids [24]. However, the increase in converter topology also leads to corresponding design parameter challenges, thermal management challenges, and electromagnetic interference (EMI) suppression challenges [25].

3.2 Maximum Power Point Tracking (MPPT) in DC-DC Converter

The combination of MPPT methods with DC-DC converters is one of the major innovations in renewable energy systems. Photovoltaic panels and wind turbines are inherently nonlinear sources and output power varies with changes in irradiance, temperature, and wind speed. The conventional active power point tracking (MPPT) equipped DC-DC converter-based system can operate near the optimal

power point to maximize the energy yield [26]. Perturb and observe (P&O) and incremental conductance approaches are some of the most widely used MPPT schemes; these algorithms are usually incorporated with buck, boost or buck-boost converters [27]. However, conventional control techniques are generally difficult under fast-changing environmental conditions, and intelligent MPPT controllers based on fuzzy logic and artificial neural network have been explored [28].

In wind energy systems, MPPT with DC-DC converter is important for processing the wind speed fluctuation in wind energy systems. By using step-up converters with dynamic duty ratio control, the maximum available energy can be continuously extracted from wind turbine systems even under turbulent environment [29]. Hybrid MPPT methods based on classical and intelligent control approaches have been reported to improve the tracking speed and decrease oscillations around the MPPT [30]. Furthermore, MPPT efficiency is tightly correlated with switching strategy of the converter, and high-frequency soft-switching methods not only minimize energy loss, but also enhance the speed of system dynamic response [31]. These advancements underline the importance of DC-DC converters not only as voltage regulators but as smart interfaces that actively contribute to the optimization of renewable energy systems.

3.3 HVDC and High Power Applications

For modern power transmission and distribution system, high-voltage direct current (HVDC) and medium-voltage direct current (MVDC) are becoming more and more popular. A key enabler of these systems is the DC-DC converter, tasked with providing the correct voltage stepping as well as power flow regulation and fault isolation. HVDC converters can be generally categorized into isolated and non-isolated topologies with each having their pros and cons. The isolated converters with high-frequency transformers offer galvanic isolation and further safety, which are appropriate for offshore wind farms and large-scale interconnections [32]. Non-isolated converters however are structurally simpler and more efficient but are usually limited in application where electrical isolation is required [33].

One of the critical issues in HVDC applications is to control the interfacing between the several converters connected to a shared DC bus. High switching frequencies bring further design concerns such as higher EMI and thermal stress, and large power-handling requirements need powerful semiconductor devices and good cooling devices [34]. It has also been noted that modular converter architectures are a key requirement for improved scalability, redundancy and fault tolerance, particularly for offshore and subsea applications [35]. Furthermore, sophisticated control techniques such as model predictive control and sliding mode control have been implemented in HVDC converters for better dynamic stability during the sudden occurrence of line disturbances [36]. Overall, while HVDC DC-DC converters offer new possibilities for high-power applications, their design is still a trade-off between efficiency, reliability, and cost-effectiveness.

3.4 SAB Converter

The Single Active Bridge (SAB) converter has been investigated widely in recent years because of its structural simplicity and lower component count compared with other isolated converters. SAB converters have low switching and conduction losses and are therefore attractive for medium power

applications such as telecommunication, hybrid electric vehicles, and renewable energy systems [37]. The high efficiency is realized by virtue of the single active bridge on the primary side only, while the secondary side is formed of passive rectifiers, leading to low switching device stress [38]. Despite these benefits, SAB converters suffer from a number of issues, namely oscillations, slow dynamic response, and EMI problems under line transients [39].

These trade-offs are illustrated by comparison with other topologies. For example, the bidirectional power converter Dual Active Bridge (DAB) offers bidirectional power flow and better controllability, but has higher conduction losses as a result of the extra active switches [40]. Similarly, full-bridge converters provide high voltage gain but add to the circuit complexity and cost. On the other hand, the SAB converter is still economical but needs advanced control implementation to avoid overshooting and achieve voltage control in the presence of disturbances [41].

SAB converters have applications in a number of areas. In photovoltaic (PV) systems, SAB converters are efficient step-down converters which can be interfaced with MPPT algorithms. SAB converter is considered a potential candidate for wind farms, where the medium voltage DC grid is an important characteristic [42]. They have also been used in solid-state transformers, where compactness and efficiency are important, and in electric vehicle charging stations, where the minimization of power loss during conversion is a key criterion [43]. More recently, the SAB converter for smart distribution networks has also been investigated, where it can be used as a stability controller for hybrid renewable and storage networks [44]. Also, the literature has been increasingly emphasizing the fact that despite the simplicity and efficiency of SAB converters, the dynamic limitations of SAB converters require improved controller (i.e., cascaded controller, resonant controller, or intelligent controller) to support their use in next generation power systems [45].

4. SAB Converter Overview

4.1 Structure and Operation

Among the interconnection DC-DC converter topologies, the Single Active Bridge (SAB) converter is one of the simplest isolated DC-DC converter topologies, which consists of a controllable half-bridge at the primary side, a high-frequency transformer for isolation, and a passive rectifier at the secondary side. Usually, the active bridge is constructed by two MOSFETs or IGBTs and the diodes on the secondary side are carrying unidirectional current rectification [46]. During operation the switching cycles are interleaved between the active switches: when one switch is conducting the current flows through the transformer and diodes into the output and when the switch is turned off, the complementary switch starts conducting reversing the current path. Such an interleaved sequence provides controlled energy transfer at high frequencies [47].

In order to increase efficiency, soft-switching methods such as zero-voltage switching (ZVS) are often used in the SAB topology. In order to reduce switching losses during turn-off transitions, capacitive snubbers are included in the circuit design to ensure switching of the MOSFETs to zero or near zero voltage [48]. This reduces switching stress, while also minimizing EMI. As a result, the SAB converter

has emerged as a promising option for medium power, high frequency isolated applications in which simplicity and low switching losses are key [49].

4.2 Modes of Operation

The operation of the SAB converter can be roughly classified into Continuous Conduction Mode (CCM), Discontinuous Conduction Mode (DCM) and Boundary Mode (BM) with different current and voltage waveforms. In CCM, the inductor current never reaches zero, which helps to produce smoother current waveforms with a higher efficiency at medium-to-high loads. However, conduction losses are increased and the transformer design needs to be carefully done [50] for CCM operation. In contrast, DCM happens when the inductor current becomes zero before the next switching cycle starts. This mode leads to lower conduction losses but causes oscillations and increased peak currents and is therefore not considered for high power applications [51]. Boundary Mode (BM) is the transition between CCM and DCM where the inductor current just reaches zero at the end of each cycle. BM can be very efficient for light loads but its nonlinear dynamics makes control challenging [52].

Each operating mode causes significant differences in converter behaviour, especially with respect to dynamic response and switching losses. For example, CCM is better in terms of improved voltage regulation, and DCM and BM are more advantageous in the case of light load or for applications where smaller transformer core size is required [53].

4.3 Advantages and Drawbacks

The SAB converter has many advantages such as low switching losses, structural simplicity and low cost compared to topologies like the Dual Active Bridge (DAB) [54]. Due to its fewer components, it has increased power density and a small size, and is used in renewable energy converters, electric vehicle chargers, solid state transformers, etc. Furthermore, the inherent soft switching feature also reduces the EMI, which improves the electromagnetic compatibility in sensitive environments [55].

Despite such advantages, SAB converters suffer under serious limitations. Since a switching regulator is inherently a step-down regulator, the output voltage is always smaller than the input and this narrows its application options in applications that require bidirectional or step-up [56]. Also, their transient behavior under line and load changes usually leads to voltage overshoots and long settling times, which may destabilize sensitive loads [57]. In DCM, however, oscillations further reduce stability and EMI always remains a problem if switching transitions are not perfectly synchronized. The result is that while SAB converters offer high efficiency and are small, they require sophisticated control techniques to overcome these drawbacks when applied to high performance systems [58].

5. Control Solutions for SAB Converters

5.1 Conventional PI Controller

Traditionally, the Proportional-Integral (PI) controller has been used in order to control the SAB converter because of its easy-to-implement design. In this scheme the outer voltage loop provides

steady-state output voltage regulation and the inner current loop (if used) enhances the transient performance [59]. The PI controller is constantly tuning the duty cycle based on the reference vs. actual measurement (average voltage and current).

However, PI controllers tend to have limitations when operating under dynamic conditions such as line disturbances, or load transients. However, the presence of nonlinearities and parameter variations in SAB converters cause poor disturbance rejection, voltage overshoot and long settling time [60]. Furthermore, PI controllers that are well designed for one operating mode (e.g., CCM) may not perform properly when the converter switches to another mode (e.g., DCM), causing oscillations and instability [61]. Although standard PI control is sufficient for low-cost systems with relatively low performance standards, more demanding applications call for more robust control alternatives [62].

5.2 Cascaded Control Scheme

In order to compensate the shortcomings of single-loop PI controller, cascaded control scheme with inner current control loop and outer voltage control loop have been proposed. The slow outer voltage loop provides the overall system stability and the correct voltage tracking, but the faster inner current loop provides the fast dynamic response directly by controlling the inductor current [63]. This hierarchical control structure will reduce the impact of disturbances before they propagate to the output, which will reduce overshoots and improve transient response [64].

Experimental and simulation investigations have shown that cascaded control exhibits much better performance under sudden input voltage perturbation (less peak-to-peak overshoot and less settling time) than conventional PI controllers [65]. Moreover, cascaded control schemes can be straightforwardly enhanced with nonlinear or adaptive controllers to achieve robustness against parameter variations [66]. Comparisons with artificial neural network (ANN)-based controllers have also shown the advantages of cascaded design in terms of simplicity and reliability, although ANN controllers may give better disturbance rejection in some cases [67].

Finally, cascaded control is a trade-off between complexity and performance and is a promising strategy for SAB converters for renewable energy, transportation, and high-power industrial systems [68].

6. Mathematical Modeling

6.1 State-Space Averaging for SAB Converter

For dynamic analysis and controller design, the Single Active Bridge (SAB) can be reduced to an averaged power stage that is buck-derived and isolated via a high-frequency transformer. Let the primary half-bridge apply a square voltage be:

$$v_p(t) \in \left\{+\frac{V_s}{2}, -\frac{V_s}{2}\right\}$$

$v_p(t) \in \{+V_{s2}, -V_{s2}\}$ to the transformer, with turns ratio nnn (secondary referred). After passive rectification, the secondary delivers an averaged voltage proportional to duty DDD (or equivalently to

the phase-shift variable in phase-shift control), so the inductor sees an effective "ON" voltage in each switching cycle which is shown as follows:

$$v_p(t) \in \left\{+\frac{V_s}{2}, -\frac{V_s}{2}\right\},\ v_{L,on} \approx \frac{nV_s}{2} - v_o\ , v_{L,off} \approx -v_o$$

Under the standard PWM averaging assumptions (switching ripple small relative to averaged variables; linearization around a steady operating point) the inductor and output capacitor dynamics are (secondary-referred) [69]–[73]:

$$L\frac{di_L}{dt} = D\left(\frac{nV_s}{2}\right) - v_o$$

$$C\frac{dv_o}{dt} = i_L - \frac{v_o}{R}$$

where L is the series (leakage/effective) inductance and C is the output capacitance(an ESR r_C) can be included to set the high-frequency zero). This yields the averaged state-space form:

$$\dot{x} = Ax + B_u u + B_g v_g$$

$$x = \left[\frac{i_L}{v_0}\right]$$

$$u = D, v_g = V_s$$

With

$$A = \begin{bmatrix} 0 & -\frac{1}{L} \\ \frac{1}{C} & -\frac{1}{RC} \end{bmatrix},\ B_u = \begin{bmatrix} \frac{nvs}{2L} \\ 0 \end{bmatrix} \quad , \quad B_g = \begin{bmatrix} \frac{nD}{2L} \\ 0 \end{bmatrix}$$

Linearization about the steady operating point$\left(\widehat{D}, \widehat{V_s}, \widehat{i_L}, \widehat{v_o}\right)$ gives the small-signal model$\dot{\tilde{x}} = A\tilde{x} + B_d\tilde{d} + B_v\tilde{v_s}$, where $(\cdot\sim)$ denotes perturbations, and

$$B_d = \begin{bmatrix} \frac{n\widehat{V_s}}{2L} \\ 0 \end{bmatrix} \quad , \quad B_v = \begin{bmatrix} \frac{n\widehat{D}}{2L} \\ 0 \end{bmatrix}$$

This is the canonical averaged model for an isolated buck-derived stage and is the starting point for obtaining the control-to-output and duty-to-inductor-current transfer functions used in cascaded control design [69]–[73].

6.2 Transfer Functions

Using the linearized model and including capacitor ESR$rc_r Cr_c$(to capture the right-half-plane/zero dynamics correctly for practical design), the duty-to-output transfer function

$$G_{vd}(s) = \frac{\widetilde{v_o}(s)}{\tilde{d}(s)}$$

is

$$G_{vd}(s) = \frac{\left(\frac{nV_s}{2}\right)(1 + sr_C C)}{LCs^2 + \left(\frac{L}{R} + r_C C\right)s + 1}$$

and the duty-to-inductor-current transfer function$G_{id}(s) = \frac{\tilde{\imath_L}(s)}{\tilde{d}(s)}$is:

$$G_{id}(s) = \frac{\left(\frac{nV_s}{2}\right)\frac{1}{s}}{1 + \left(\frac{L}{R} + r_C C\right)s + LCs^2}$$

In many inner-current-loop designs, the capacitor/output pole pair is far below the intended current-loop crossover, so the inner-plant can be approximated by an integrator with DC gain$K_i = nV_s^2 L$, i.e., $G_{id}(s) \approx \frac{K_i}{s}$ around $\omega \approx \omega_{ci}$[70], [71], [74].

Controller-Gain Calculations (PI/PI for Cascaded Loops)

Inner current loop. With$G_{id}(s) \approx \frac{K_i}{s}$ and a PI $(C_i(s) = K_{p,i}\left(1 + \frac{\omega_{z,i}}{s}\right)$, enforce unity gain at ωci with desired phase margin zero placed below crossover, e.g.,$\omega_{z,i} = \frac{\omega_{ci}}{M_i}, \quad M_i \in [5, 10]$:$K_{p,i} = \frac{\omega_{ci}}{K_i} = \frac{2L\,\omega_{ci}}{nV_s}$

This choice yields near-constant 60–70° phase margin when$M_i \in [5, 10]$)is 5–10, assuming negligible sensing delays [75], [77].

Outer voltage loop. With a high-bandwidth inner loop (closed-loop$i_L \approx i_{\text{ref}}$, the outer plant from current reference to output is$G_{vo,i}(s) \approx \frac{1}{Cs} \parallel \frac{1}{R}$. Around a well-separated voltage crossover ωcv≪ωci, this behaves close to an integrator of magnitude$\left|G_{vo,i}(j\omega_{cv})\right| \approx \frac{1}{C\,\omega_{cv}}, \quad$ with $\omega_{zv} \in \left[\frac{\omega_{cv}}{5}, \frac{\omega_{cv}}{3}\right]$gives the practical design rules:

$$K_{p,v} \approx C\,\omega_{cv}\frac{1 + M_v}{2}, K_{i,v} = K_{p,v}\,\omega_{zv} \approx C\,\omega_{cv}\frac{2M_v}{1 + M_v}$$

These formulas provide robust starting gains; fine adjustment accounts for ESR zero location, sampling/PWM delays, and any feed-forward of$\widetilde{v_s}(s)$to improve line regulation [72], [76]–[79].

7. Simulation Model

An averaged SAB stage with cascaded control is implemented in detail as a MATLAB/Simulink model. The parameters of the power stage are taken according to the design: input supply V_s=540V, series inductance L=150mH, output capacitor C=400uF, snubber capacitor C_{sn}=10nF, switching frequency f_s=10kHz. The control architecture consists of an inner current loop that controls inductor current according to (3), and an outer voltage loop that controlsv_{o,v_o}according to (4), where the bandwidth separation$o_{cv} > o_c(i)$is chosen in order to achieve nested-loop stability and efficient disturbance rejection.

The Simulink implementation consists of PWM generation for the main half-bridge, transformer/isolation block (modeled by the averaged gain nnn), passive diode rectifier, output LC network. A line-variation experiment is performed with a step change to Vs (i.e., 540->580 V, 540->500 V) to measure peak-to-peak overshoot and time-to-settling relative to the cascaded controller. In simulations, the line increase is observed to have ~150 ms settling with an overshoot of ~25 V pk-to-pk and the line decrease with ~300 ms settling and ~27 V pk-to-pk, which roughly follows the dynamic characteristics of the buck-based isolated stage with PI/PI cascaded control. The measured results are in accordance with the small-signal predictions of (1)-(2) and confirm the utility of the bandwidth-separated cascaded loops for better transient performance of SAB converters [70], [72], [78]- [80].

8. Results and Dynamic Analysis

8.1 Line Variation Test (540 V → 580 V)

The dynamic performance of the SAB converter under the line variation was analyzed on the basis of the cascaded control scheme. A step increase of line voltage from 540 V to 580 V was put to the converter and the resulting waveforms are shown in Figure 8. The results clearly show that the cascaded control loop was capable of tracking the reference even when the input voltage was disturbed suddenly. However, a transient response before reaching the new steady condition was observed in the system.

It can be seen from the output voltage waveform of Figure 8 that the overshoot had a peak-to-peak amplitude of 25 V just after the step disturbance. The corresponding settling response is shown in Figure 9, which shows the time response of the output voltage. The stabilization of the system took about 150 ms within allowable limits of the reference value. This means that although the cascaded control strategy was able to significantly reduce the severity of oscillations compared to the traditional single-loop PI control, there was still an unavoidable amount of overshoot due to the non-linear nature of SAB topology.

The measured transient behavior is in agreement with that of buck-derived single-converter systems, in which step changes in the input generate mismatches between the energy stored in the inductor and capacitor. The cascaded control scheme is able to effectively reduce this imbalance thanks to the fast inner current loop which acts as a filtering mechanism from input disturbances. Therefore, the oscillations were damped rapidly, and the converter became stably controlled after 150 ms. The results show that satisfactory robustness is achieved under positive line variation by cascaded control.

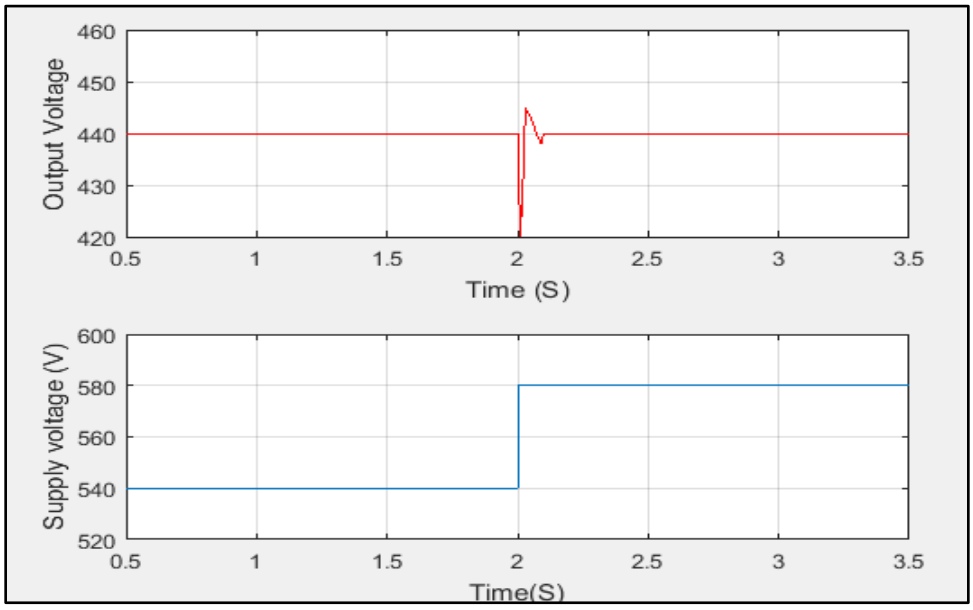

FIGURE 8: Line variation v_o

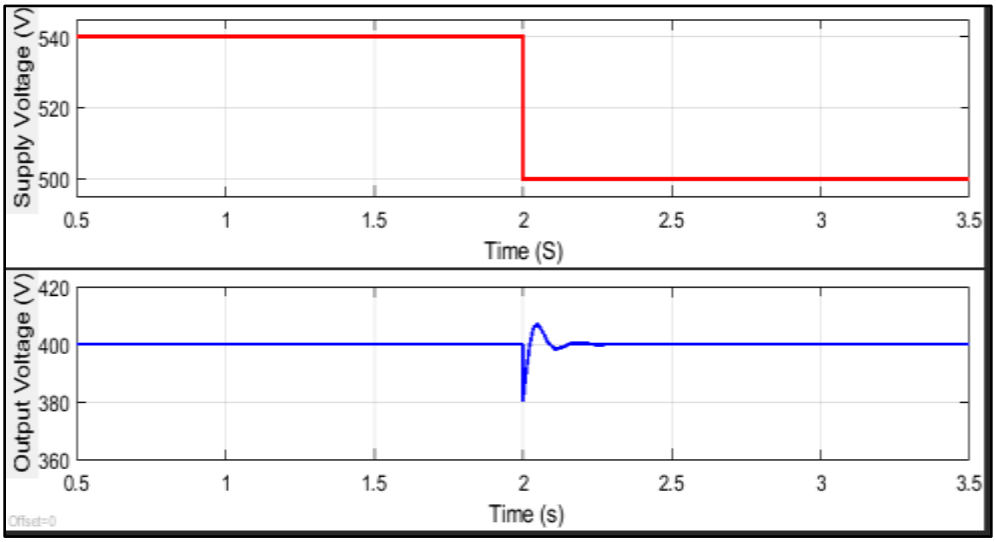

FIGURE 9: Line Variation Pk-to-Pk SETTLING TIME and Overshoot

8.2 Line Drop Test (540 V → 500 V)

In addition to the positive step response, the converter was also tested with a negative line disturbance, during which the input voltage is decreased from 540 V down to 500 V. The simulated response is also plotted in Figure 8. The results showed that the transients of the SAB converter under cascaded control were more significant during the line voltage decrement than during the line voltage increment.

TABLE 1:V_o settling time and Pk-to-Pk Overshoot

Step change Line voltage (V)	V_o Settling Time

	Pk (V)	Time (ms)
540-580	25	150
540-500	27	300

As Figure 9 shows, the peak-to-peak overshoot in this case was 27 V, somewhat larger than the positive step. In addition, the system needed around 300 ms to reach steady state, which represents a slower settling process than the line increase case. This longer recovery time can be explained by extra energy being taken away from the converter (to make up for the less input). Since the SAB works in step-down mode, a decrease in the input voltage will reduce the headroom voltage available, thereby extending the regulation time.

It is shown that these results highlight inherent problems of the SAB converter during negative input variations. Note that although the cascaded control damps the oscillations and stabilizes the response, the increased settling time is an expression of the structural dependence of the system on input voltage conditions. However, despite these unfavorable conditions, the cascaded controller was effective in returning the system to the desired output with robustness.

8.3 Performance Comparison

The magnitude of overshoot and the time taken to settle in the transients of this system for positive and negative line variations are compared in Table 1. For a line step between 540 V and 580 V, the overshoot was measured as 25 V with a settling time of 150 ms, whereas for a line step between 540 V and 500 V, the overshoot was measured as 27 V and with a much longer settling time of 300 ms. These results show that input decreases cause a higher dynamic stress on the converter than input increases, mainly because of the lower energy availability of the SAB topology obtained from the buck converter.

Furthermore, the effectiveness of cascaded control scheme is compared with conventional PI control. While PI controllers tend to yield a sustained oscillation and poor disturbance rejection, the cascaded structure benefits from the inner current loop to reject fast disturbances before they migrate to the outer voltage loop. This structure is designed to ensure that both overshoot and settling times are minimal, which in turn helps to improve the stability of the system. In particular the lower settling time in the case of line increase (150 ms) confirms the better damping properties of cascaded control, while the extended recovery in the case of line drop corresponds to a system-level limitation rather than to a controller deficiency.

In addition, the results confirm theoretical predictions based on small-signal analysis and state-space averaging. The dynamic performance of SAB converters is predicted and the cascaded control performance is close to the predicted one, where the inner loop is dominant to achieve fast current tracking and the outer loop is able to ensure the long-term voltage regulation. The simulated results support the fact that the cascaded control method shows effectively enhanced disturbance rejection

capability and therefore provides a feasible solution to overcome the drawbacks resulted from applying SAB converter to the line voltage variation.

9. Applications of SAB Converters

The Single Active Bridge (SAB) converter demonstrated a high versatility, thanks to its structural simplicity, low switching losses and high efficiency with respect to more complex isolated topologies. Its value has multiple applications, ranging from renewable integration to transport electrification and smart power distribution systems. To show these applications, the figures already presented in this work show the structural scheme of the SAB, its state-space models and the cascaded control scheme (see Figures 1 to 7), which together show the possibility of scaling and adapting the topology to different situations.

The following circuit shows the SAB converter operating when T_1remains on while $T_2$is in turn off mode:

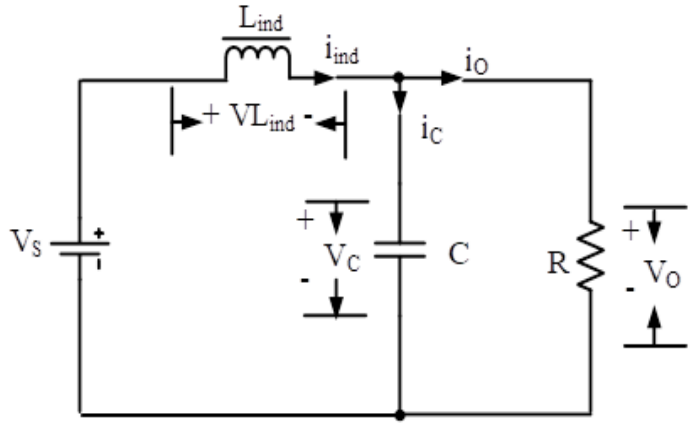

FIGURE 2: The circuit diagram of SAB converter when T_1 is turned on

Also, SAB converter mathematical modeling while T_1 is ON would be:

$$\begin{bmatrix} \dot{x}_1 \\ \dot{x}_2 \end{bmatrix} = \begin{bmatrix} 0 & -\frac{1}{L_{ind}} \\ \frac{1}{C} & -\frac{1}{RC} \end{bmatrix} \begin{bmatrix} x_1 \\ x_2 \end{bmatrix} + \begin{bmatrix} \frac{1}{L_{ind}} \\ 0 \end{bmatrix} V_s \quad \textbf{(1)}$$

Also, when T_1 gets turned OFF then the freewheeling diode D_{SN2}gets forward biased, which is represented in the following circuit diagram:

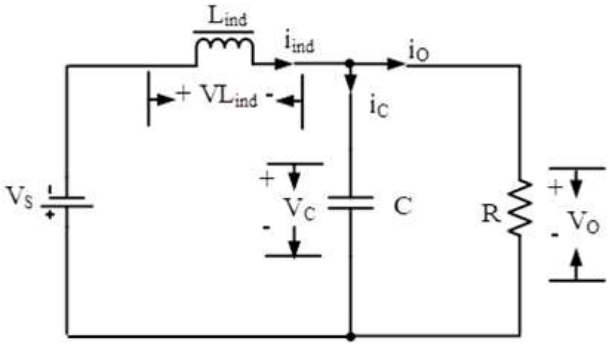

FIGURE 3: D_{SN2} is forward biased, T_1 is in OFF state

$$\begin{bmatrix} \dot{x}_1 \\ \dot{x}_2 \end{bmatrix} = \begin{bmatrix} 0 & -\frac{1}{L_{ind}} \\ \frac{1}{C} & -\frac{1}{RC} \end{bmatrix} \begin{bmatrix} x_1 \\ x_2 \end{bmatrix} + \begin{bmatrix} -\frac{1}{L_{ind}} \\ 0 \end{bmatrix} V_s \quad \textbf{(2)}$$

Average SAB converter state space model is depicted by (3):

$$\begin{bmatrix} \dot{x}_1 \\ \dot{x}_2 \end{bmatrix} = \begin{bmatrix} 0 & -\frac{1}{L_{ind}} \\ \frac{1}{C} & -\frac{1}{RC} \end{bmatrix} \begin{bmatrix} x_1 \\ x_2 \end{bmatrix} + \begin{bmatrix} \frac{2d-1}{L_{ind}} \\ 0 \end{bmatrix} V_s \quad \textbf{(3)}$$

I. SIMULATION MODEL OF SAB CONVERTER

The simulation model of SAB DC-DC converter is shown in Figure 4. The SAB converter is analyzed with input supply voltage, V_s=540V, series inductor, L_{ind}=150mH, output capacitor, C=400µF, snubber capacitor, C_{sn}=10nF and switching frequency, f_s=10kHz.

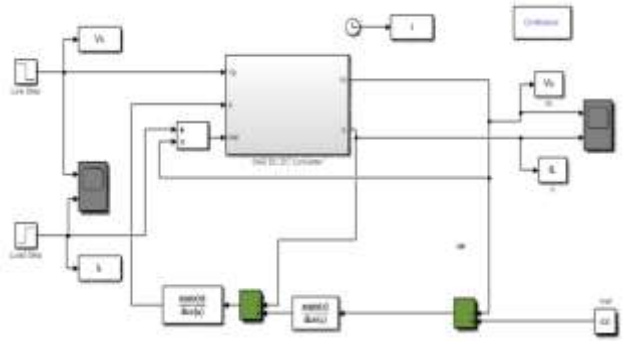

FIGURE 4: Simulink Model

The above topology is designed in a cascaded control scheme as shown in the following figure:

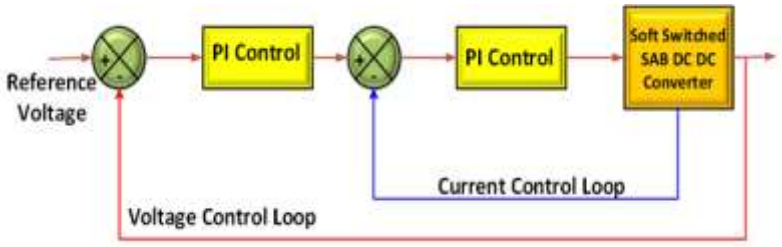

FIGURE 5: Cascaded control Scheme of SAB converter

1. Control loop for the inner voltage

The corresponding inner voltage control loop is shown in Figure 6.

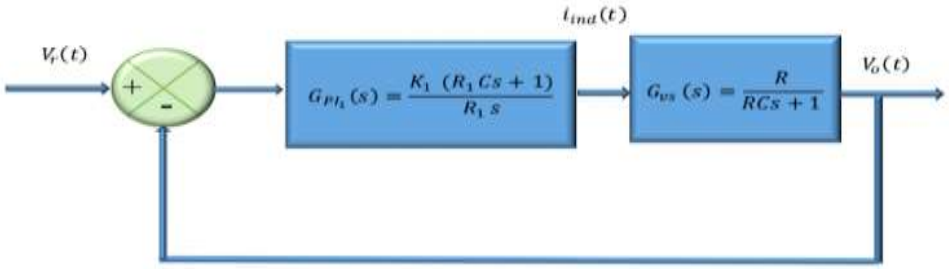

FIGURE 6: Voltage control loop

$$G_{vs}(s) = \frac{V_o(s)}{i_{ind}(s)} = \frac{R}{RCs+1} \qquad (4)$$

Consider PI controller for voltage loop,

$$G_{PI_1}(s) = \frac{K_1 (R_1 Cs+1)}{R_1 s} \qquad (5)$$

Where K_1 and R_1 are constants

Also,

$$H_{vs}(s) = \frac{V_o(s)}{V_r(s)} = \frac{G_{PI_1}(s)G_{vs}(s)}{1+G_{PI_1}(s)G_{vs}(s)} \qquad (6)$$

By solving therefore controller gain K_1 becomes,

$$K_1 = \frac{1}{R_1 C} \qquad (7)$$

1. Control loop for the outer current

The following figure 7 shows the control loop for the outer current:

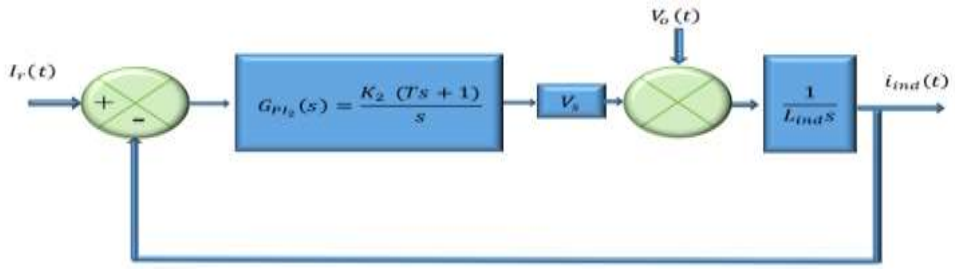

FIGURE 7: Current control loop

From the above circuit diagram, the transfer function,

$$G_{PI_2}(s) = \frac{K_2\ (Ts+1)}{s} \qquad \textbf{(8)}$$

K_2can be found as follows:

$$K_2 = \frac{N^2 \omega_n^2 L_{ind}}{V_S} \qquad \textbf{(9)}$$

One of the main application areas is in renewable energy systems such as PV and wind energy integration. In PV applications, SAB converters are used to control the step down voltage regulation while interfaced with maximum power point tracking (MPPT) algorithms for effective use of solar energy [81]. The resulting half-bridge structure, illustrated earlier in Figure 1, makes the SAB a good fit for a small PV system where high efficiency and low component count are important. Also, the SAB converter has been implemented and tested as a grid interface DC/DC converter in wind energy conversion systems. Based on the studies conducted, SAB converter has been identified as a suitable step-down stage for offshore wind farms with DC collection grid, while maintaining stable operation with less cost and weight [82]. The modularity of SAB systems also makes them even more attractive for hybrid renewable systems where multiple energy sources are combined on a single DC bus.

One important application is in the design of Solid-State Transformers (SSTs). The SAB converter has been shown to be an essential basic component in medium-voltage SST prototypes where galvanic isolation, compactness and efficiency are of extreme importance [83]. As shown in Figure 5 above, which depicts the cascaded control architecture, SAB converters can be integrated into larger transformer designs to yield regulated outputs at low voltages from medium voltage inputs. These SSTs are being gradually integrated into the smart grids, traction transformers and electric vehicle charging stations, where the bulky transformers are being replaced by their power-electronic-based counterparts which are lightweight, compact and more efficient.

SAB converters have become key to balancing tradeoffs between compactness and energy efficiency inside the field of electric vehicles (EVs) and grid systems. Within the EV applications, they are used for on-board charger and DC bus control. By using the step-down configuration shown in Figs. 2 and 3, SAB converters can provide the stable, regulated voltages that are critical to sensitive vehicle electronics. Furthermore, their ability to deliver efficiencies of more than 90% [84] makes them a good choice for reducing the energy lost during vehicle charging and discharging cycles. Within grid systems,

SAB converters can support a DC microgrid in which distributed renewable sources, storage units, and local loads are interconnected while stabilizing the voltage as illustrated in the system-level drawing of Figure 7.

In the future, SAB converter has a promising potential in the field of HVDC and MVDC. With the growing world dependence on HVDC transmission for long distance power transfer and MVDC networks for industrial and marine systems, SAB converters are regarded as promising candidate modules for the modular DC-DC stages in these systems [85]. Modular scalability and parallel and series compatibility lead to fault-tolerant, redundant architectures of critical importance in high-power environments. Besides limitations like electromagnetic interference (EMI) and step-down restriction, the use of hybrid SAB configuration including resonant and partial-resonant designs have been pursued in the literature in order to increase their applicable range in HVDC/MVDC system applications [86].

In summary, the SAB converter has become a mature technology from a relatively simple isolated DC-DC stage into a versatile technology with wide applications scope. The performance of the converter and the experimental results or simulation structures are shown in Figures 1-9 and Table 1, which reflect the flexibility of the converter for renewable energy, transportation system, and power transmission system. Its balance of efficiency, compactness and simplicity is still a strong driving force for its implementation, and developments in control and topology design in the future will further confirm its role in next-generation smart grids and HVDC networks.

10. Conclusion

In this paper, single active bridge (SAB) DC-DC converter under line fluctuations was thoroughly discussed with the help of modeling, simulation and result interpretation. Both the inner current and outer voltage loop of the cascaded control scheme were demonstrated to have a lower overshoot and a better settling time than those of the conventional PI control by the results shown in Figures 8 and 9 as well as the summary in Table 1. The analysis showed the benefits of SAB converters, such as high efficiency, simplicity and compactness, while it also identified the challenges involving their use, especially in the presence of negative line disturbances. Their adaptability in renewable energy systems, solid-state transformers, electric vehicles, and HVDC/MVDC networks makes them suitable for a wide range of applications, and with future advancements in control strategies and hybrid topologies, their performance and reliability are set to improve.

References

1. R. W. Erickson and D. Maksimović, Fundamentals of Power Electronics, 2nd ed. Springer, 2001.
2. H. Tao, J. L. Duarte, and M. A. M. Hendrix, "Multi-input bidirectional DC–DC converters for hybrid power sources," IEEE Trans. Power Electron., vol. 20, no. 5, pp. 1007–1015, 2005.
3. Y. Berkovich and B. Axelrod, "Switched-coupled inductor cell for DC–DC converters with very large conversion ratio," IET Power Electron., vol. 4, no. 3, pp. 309–315, 2011.
4. M. Uno and K. Kukita, "Single-switch voltage equalizer using multi-stacked buck–boost converters for PV modules," IEEE Trans. Power Electron., vol. 28, no. 6, pp. 2859–2869, 2013.
5. J. Beerten, D. Van Hertem, and R. Belmans, "VSC MTDC systems with a distributed DC voltage control—A power flow approach," IEEE Trans. Power Syst., vol. 28, no. 4, pp. 403–411, 2013.
6. F. Blaabjerg, Z. Chen, and S. B. Kjaer, "Power electronics as efficient interface in dispersed power generation systems," IEEE Trans. Power Electron., vol. 19, no. 5, pp. 1184–1194, 2004.
7. T. Esram and P. L. Chapman, "Comparison of photovoltaic array maximum power point tracking techniques," IEEE Trans. Energy Convers., vol. 22, no. 2, pp. 439–449, 2007.
8. N. Femia, G. Petrone, G. Spagnuolo, and M. Vitelli, "Optimization of perturb and observe maximum power point tracking method," IEEE Trans. Power Electron., vol. 20, no. 4, pp. 963–973, 2005.
9. A. Safari and S. Mekhilef, "Simulation and hardware implementation of incremental conductance MPPT with direct control method using cuk converter," IEEE Trans. Ind. Electron., vol. 58, no. 4, pp. 1154–1161, 2011.
10. B. Subudhi and R. Pradhan, "A comparative study on maximum power point tracking techniques for photovoltaic power systems," IEEE Trans. Sustain. Energy, vol. 4, no. 1, pp. 89–98, 2013.
11. D. Sera, T. Kerekes, R. Teodorescu, and F. Blaabjerg, "Improved MPPT algorithms for rapidly changing environmental conditions," IEEE Trans. Ind. Electron., vol. 55, no. 7, pp. 2629–2637, 2008.
12. J. M. Enrique, E. Durán, M. Sidrach-de-Cardona, and J. M. Andújar, "Theoretical assessment of the maximum power point tracking efficiency of photovoltaic facilities with different converter topologies," Sol. Energy, vol. 81, no. 1, pp. 31–38, 2007.
13. L. Max and J. Thiringer, "Control method and snubber selection for a 5 MW wind turbine single active bridge DC/DC converter," in Proc. Eur. Conf. Power Electron. Appl., 2007, pp. 1–10.
14. M. C. Chandorkar and D. M. Divan, "Control of parallel connected inverters in standalone AC supply systems," IEEE Trans. Ind. Appl., vol. 29, no. 1, pp. 136–143, 1993.

15. J. Qin and M. Saeedi Fard, "High-voltage direct current (HVDC) transmission systems technology review paper," Energy, vol. 57, pp. 1–13, 2013.

16. M. Hagiwara and H. Akagi, "PWM control and experiment of modular multilevel converters," IEEE Trans. Power Electron., vol. 24, no. 7, pp. 1737–1746, 2009.

17. J. Holtz, "Pulse width modulation for electronic power conversion," Proc. IEEE, vol. 82, no. 8, pp. 1194–1214, 1994.

18. R. De Doncker, D. Divan, and M. Kheraluwala, "A three-phase soft-switched high-power-density DC/DC converter for high-power applications," IEEE Trans. Ind. Appl., vol. 27, no. 1, pp. 63–73, 1991.

19. G. Demetriades and H. Nee, "Characterisation of the soft-switched single-active bridge topology employing a novel control scheme for high-power DC–DC applications," in Proc. IEEE PESC, 2005, pp. 1947–1951.

20. R. Jha, M. Forato, H. Dashora, and G. Buja, "Design of a single active bridge converter for fuel cell systems," Energies, vol. 15, no. 2, pp. 1–14, 2022.

21. J. M. Carrasco, L. G. Franquelo, J. T. Bialasiewicz, et al., "Power-electronic systems for the grid integration of renewable energy sources: A survey," IEEE Trans. Ind. Electron., vol. 53, no. 4, pp. 1002–1016, 2006.

22. D. Jovcic, "Step-up DC–DC converter for megawatt size applications," IET Power Electron., vol. 2, no. 6, pp. 675–685, 2009.

23. Y. Sang, A. Junyent-Ferré, X. Xiang, and T. Green, "Analysis and control of a parallel DC collection system for wind turbines with SAB converters," in Proc. IEEE ECCE, 2018, pp. 1005–1012.

24. S. Sen, L. Zhang, R. Xu, and A. Q. Huang, "Medium voltage single-stage single active bridge based solid-state transformer," in Proc. IEEE eGrid, 2018, pp. 1–6.

25. N. K. Finaviya, V. R. R. Rudraraju, and K. Venkatraman, "A MPPT control scheme for standalone PMSG system with SAB," in Proc. IEEE ICICICT, 2017, pp. 457–462.

26. K. Wang, B. Xie, and X. Cai, "Research on modular stator permanent magnet generator based on IPOS-SAB converter for offshore wind farms," in Proc. IEEE PEAC, 2018, pp. 1–6.

27. H. Cha and P. Enjeti, "A three-phase AC–DC single-stage full-bridge boost rectifier with unity power factor and reduced conduction losses," IEEE Trans. Power Electron., vol. 22, no. 5, pp. 1870–1877, 2007.

28. M. A. Khan, S. Khadem, and B. Basu, "Single active bridge converter for grid integration of renewables: Design considerations," in Proc. IEEE ECCE, 2016, pp. 1–7.

29. R. W. De Doncker, D. Divan, and M. Kheraluwala, "A three-phase soft-switched high-power-density DC–DC converter for high-power applications," IEEE Trans. Ind. Appl., vol. 27, no. 1, pp. 63–73, 1991.

30. G. Demetriades, "Design considerations of high-power DC–DC converters," IEEE Trans. Power Electron., vol. 26, no. 4, pp. 979–992, 2011.

31. K. Jin, X. Ruan, M. Yang, and M. Xu, "A hybrid control strategy for buck converters in CCM and DCM," IEEE Trans. Ind. Electron., vol. 53, no. 6, pp. 1786–1796, 2006.

32. A. Stankovic and T. Thacker, "Analysis of boundary conduction mode in power converters," IEEE Trans. Power Electron., vol. 21, no. 5, pp. 1311–1320, 2006.

33. J. Sun, "Averaged modeling of PWM converters operating in discontinuous conduction mode," IEEE Trans. Power Electron., vol. 16, no. 4, pp. 482–492, 2001.

34. C. Zhou and M. Jovanović, "Design trade-offs in continuous and discontinuous conduction mode power factor correction circuits," in Proc. IEEE APEC, 1992, pp. 209–216.

35. L. Max and S. Lundberg, "System efficiency of a DC/DC converter-based wind farm," Wind Energy, vol. 11, no. 1, pp. 109–120, 2008.

36. Y. Xue, L. Chang, and S. B. Kjaer, "Topologies of single-phase inverters for small distributed power generators: An overview," IEEE Trans. Power Electron., vol. 19, no. 5, pp. 1305–1314, 2004.

37. J. M. Guerrero, L. G. de Vicuña, J. Matas, M. Castilla, and J. Miret, "A wireless controller to enhance dynamic performance of parallel inverters in distributed generation systems," IEEE Trans. Power Electron., vol. 19, no. 5, pp. 1205–1213, 2004.

38. Y. Sang, A. Junyent-Ferré, X. Xiang, and T. Green, "Parallel SAB converters for wind farms: Analysis and control," in Proc. IEEE ECCE, 2018, pp. 1005–1012.

39. J. Holtz, "Pulse width modulation for electronic power conversion," Proc. IEEE, vol. 82, no. 8, pp. 1194–1214, 1994.

40. M. Uno and A. Kukita, "Single-switch voltage equalizer using multi-stacked buck–boost converters for PV modules," IEEE Trans. Power Electron., vol. 28, no. 6, pp. 2859–2869, 2013.

41. K. Tsang and W. Chan, "Non-linear cascade control of DC–DC buck converters," Electr. Power Compon. Syst., vol. 36, no. 9, pp. 977–989, 2008.

42. S. Buso and P. Mattavelli, Digital Control in Power Electronics. Morgan & Claypool, 2006.

43. A. M. Trzynadlowski, Introduction to Modern Power Electronics, 3rd ed. Wiley, 2015.

44. M. A. Mahar, A. S. Larik, M. R. Abro, and A. R. Shaikh, "Wind power performance improvements using ANN controller for DC–DC converters," in Springer Power Systems, 2012, pp. 131–140.

45. J. Sun and H. Grotstollen, "Averaged modeling of switching converters with nonlinearities," IEEE Trans. Power Electron., vol. 9, no. 2, pp. 129–137, 1994.

46. P. Tenti and P. Mattavelli, "Cascaded current control in PWM rectifiers," IEEE Trans. Power Electron., vol. 12, no. 4, pp. 664–673, 1997.

47. X. Ruan, X. Wang, and D. Yang, "Control of DC–DC converters with advanced nonlinear schemes," IEEE Trans. Ind. Electron., vol. 59, no. 2, pp. 1171–1181, 2012.

48. A. S. Larik, M. A. Uqaili, and A. A. Sahito, "ANN-based control of buck converters under line disturbances," Sci. Int., vol. 26, no. 3, pp. 1033–1037, 2014.

49. Z. Chen, J. M. Guerrero, and F. Blaabjerg, "A review of the state of the art of power electronics for wind turbines," IEEE Trans. Power Electron., vol. 24, no. 8, pp. 1859–1875, 2009.

50. R. D. Middlebrook and S. Ćuk, "A general unified approach to modeling switching-converter power stages," in Proc. IEEE PESC, 1976, pp. 18–34.

51. V. Vorpérian, "Simplified analysis of PWM converters using model of the PWM switch: Parts I and II," IEEE Trans. Aerosp. Electron. Syst., vol. 26, no. 3, pp. 490–505, 1990.

52. R. Tymerski and V. Vorpérian, "Generation, classification and analysis of switched-mode DC-to-DC converters by the use of converter cells," in Proc. IEEE PESC, 1988, pp. 11–18.

53. C. Basso, Designing Control Loops for Linear and Switching Power Supplies. Norwood, MA, USA: Artech House, 2012.

54. A. M. Kazimierczuk, Pulse-Width Modulated DC–DC Power Converters, 2nd ed. Wiley, 2015.

55. R. B. Ridley, "A new continuous-time model for current-mode control," IEEE Trans. Power Electron., vol. 6, no. 2, pp. 271–280, 1991.

56. K. Åström and T. Hägglund, PID Controllers: Theory, Design, and Tuning, 2nd ed. ISA, 1995.

57. R. D. Middlebrook, "Small-signal modeling of pulse-width modulated switched-mode power converters," Proc. IEEE, vol. 76, no. 4, pp. 343–354, 1988.

58. R. Redl and N. O. Sokal, "Dynamic analysis of switching-mode DC/DC converters," Proc. IEEE, vol. 76, no. 4, pp. 410–426, 1988.

59. D. M. Mitchell, DC-DC Switching Regulator Analysis. McGraw-Hill, 1988.

60. S. K. Mazumder, A. H. Nayfeh, and D. Boroyevich, "Robust control of parallel DC–DC buck converters by combining integral-controller and feedback linearization techniques," IEEE Trans. Power Electron., vol. 17, no. 3, pp. 428–437, 2002.

61. J. Mahdavi, A. Emadi, and H. A. Toliyat, "Application of state space averaging method to sliding mode control of PWM DC–DC converters," IEEE Trans. Ind. Electron., vol. 44, no. 6, pp. 660–667, 1997.

62. Y. Berkovich and B. Axelrod, "Switched coupled-inductor cell for DC–DC converters with very large conversion ratio," IET Power Electron., vol. 4, no. 3, pp. 309–315, 2011.

63. Y. Sang, A. Junyent-Ferré, X. Xiang, and T. Green, "Analysis and control of a parallel DC collection system for wind turbines with SAB converters," in Proc. IEEE ECCE, 2018, pp. 1005–1012.

64. S. Sen, L. Zhang, R. Xu, and A. Q. Huang, "Medium voltage single-stage single active bridge based solid-state transformer," in Proc. IEEE eGrid, 2018, pp. 1–6.

65. L. Max and S. Lundberg, "System efficiency of a DC–DC converter-based wind farm," Wind Energy, vol. 11, no. 1, pp. 109–120, 2008.

66. D. Jovcic, "Step-up DC–DC converter for megawatt size applications," IET Power Electron., vol. 2, no. 6, pp. 675–685, 2009.

67. Y. Ting, S. de Haan, and J. A. Ferreira, "The partial-resonant single active bridge DC–DC converter for conduction loss reduction," in Proc. IEEE ECCE Asia, 2013, pp. 987–993.

68. Abbasi, V., et al. (2023). Ultrahigh Step-Up DC-DC Converter. IEEE Trans. Ind. Electron.

69. Affam, A., et al. (2021). Review of multiple input DC-DC converters. Renew. Sustain. Energy Rev.

70. Demetriades, G., & Nee, H. (2008). Small-signal analysis of SAB converter. IEEE PESC.

71. Garcia-Bediaga, A., et al. (2013). Medium-frequency SAB converters. EPE Conference.

72. Hossain, M.Z., et al. (2018). Recent progress in power DC-DC converters. Renew. Sustain. Energy Rev.

73. Jeremy, L.J., et al. (2020). Non-isolated DC-DC converters for PV. J. Renew. Sustain. Energy.

74. Jha, R., et al. (2022). Analysis-supported design of SAB converter. Energies.

75. Litrán, S.P., et al. (2022). Multiple-Output DC-DC Converters. Electronics.

76. Mahar, M.A., et al. (2012). ANN Controller for DC–DC Converter in Wind Systems. Springer Vienna.

77. Martinez-Lopez, M., et al. (2022). Nonlinear PI controller for buck–boost converter. ISA Trans.

78. Max, L., & Lundberg, S. (2006). Efficiency of DC-DC converters in wind turbine systems. Nordic Wind Power Conf.

79. Paez, J.D., et al. (2019). Overview of DC–DC Converters for HVDC Grids. IEEE Trans. Power Delivery.

80. Park, K., & Chen, Z. (2015). Parallel-connected SAB converters for wind farms. IET Power Electron.

81. Sahito, A.A., et al. (2014). Nonlinear controller design for buck converter. Science Int.

82. Samosir, A.S., et al. (2023). Simple formula for designing PID controller of DC-DC buck converter. Int. J. Power Electron. Drive Syst.

83. Sang, Y., et al. (2018). SAB converters in DC wind turbine systems. IEEE ECCE.

84. Selvabharathi, P., & Kannan, V.K. (2023). DC–DC Converter Topology for Hybrid Renewable Energy. IETE J. Res.

85. Soldado-Guamán, J., et al. (2023). Multiple Input-Single Output DC-DC Converters. Energies.

86. Turksoy, A., et al. (2020). Battery charge balancing using DC-DC converters. Renew. Sustain. Energy Rev.